

Surface Properties of the Half- and Full-Heusler Alloys

I Galanakis §

Institut für Festkörperforschung, Forschungszentrum Jülich, D-52425 Jülich, Germany

Abstract. Using a full-potential *ab-initio* technique I study the electronic and magnetic properties of the (001) surfaces of the half-Heusler alloys, NiMnSb, CoMnSb and PtMnSb and of the full-Heusler alloys Co₂MnGe, Co₂MnSi and Co₂CrAl. The MnSb terminated surfaces of the half-Heusler compounds present properties similar to the bulk compounds and, although the half-metallicity is lost, an important spin-polarisation at the Fermi level. In contrast to this the Ni terminated surface shows an almost zero net spin-polarisation. While the bulk Co₂MnGe and Co₂MnSi are almost half-ferromagnetic, their surfaces lose the half-metallic character and the net spin-polarisation at the Fermi level is close to zero. Contrary to these compounds the CrAl terminated (001) surface of Co₂CrAl shows a spin polarisation of about 84%.

PACS numbers: 73.20.-r, 73.20.At, 71.20.-b, 71.20.Lp

Short title: Surface Properties of the Half- and Full-Heusler Alloys

October 22, 2018

§ To whom correspondence should be addressed, e-mail: I.Galanakis@fz-juelich.de

1. Introduction

After the discovery of giant magnetoresistance (GMR) by the groups of Fert [1] and Grünberg [2] in 1988, a new field in condensed matter, the magneto- or spinelectronics, evolved which has grown steadily in the last ten years. One of the most interesting problems of this new field is the spin-injection from a ferromagnet into a semiconductor, that would lead to the creation of efficient spin-filters [3], tunnel junctions [4], GMR devices for spin injection [5], etc. This has intensified the interest in the so-called half-ferromagnetic materials which have a band gap at the Fermi level (E_F) for one spin direction and thus exhibit 100% spin polarisation at E_F . So in principle during the spin-injection process only spin-up electrons would be injected in the semiconductor allowing the creation of the perfect spin-filter and spin-dependent devices with superior performances.

Attractive candidates for half-ferromagnetic materials are the Heusler alloys of which two distinct families exist. The compounds of the first family have the form XYZ and crystallize in the $C1_b$ structure, which consists of 4 fcc sublattices occupied by the three atoms X, Y and Z and a vacant site [6]. They are also known as half-Heusler compounds. In 1983 de Groot and his collaborators [7] showed that one of them, NiMnSb, has a gap at E_F in the minority band. Also PtMnSb [8, 9] and CoMnSb [10] have been predicted to be half-ferromagnets. Infrared absorption [11] and spin-polarized positron-annihilation [12] experiments have verified the half-ferromagnetic character of bulk NiMnSb. There is also ellipsometric evidence of the spin-down gap for PtMnSb [13].

Recently it has become possible to grow high quality films of Heusler alloys and it is mainly NiMnSb that has attracted the attention [14]. Unfortunately these films were found not to be half-ferromagnetic [15, 16, 17, 18]; a maximum value of 58% for the spin-polarisation of NiMnSb was obtained by Soulen *et al.* [15]. These polarisation values are consistent with a small perpendicular magnetoresistance measured for NiMnSb in a spin-valve structure [19], a superconducting tunnel junction [4] and a tunnel magnetoresistive junction [20]. Ristoiu *et al.* showed that during the growth of the NiMnSb thin films, Sb and then Mn atoms segregate to the surface, which is far from being perfect, thus decreasing the obtained spin-polarisation [21]. But when they removed the excess of Sb by a flash annealing, they managed to get a nearly stoichiometric ordered alloy surface being terminated by a MnSb layer, which presented a spin-polarisation of about $67\pm 9\%$ at room temperature [21]. The temperature dependence of the spin moments for such a film was studied by Borca *et al.* [22]. Wijs and de Groot have shown by first-principle calculations that NiMnSb surfaces do not present 100% spin-polarisation and they proposed that at some interfaces it is possible to restore the half-ferromagnetic character of NiMnSb [23]. Also recently, Jenkins and King studied by a pseudopotential technique the MnSb terminated (001) surface of NiMnSb and showed that there are two surface states at the Fermi level, which are well localized at the surface layer [24] and they persist even when the MnSb surface is covered by a Sb overlayer [25]. They found also that the surface only mildly reconstructs; the Sb atoms move outwards, the Mn atoms inwards with a total buckling of only 0.06 Å, and this small $c(1 \times 1)$ reconstruction is energetically more favourable than the creation of Mn or Sb dimers.

The second family of Heusler alloys are the so-called full-Heusler alloys and they have the X_2YZ formula. They crystallize in the $L2_1$ structure which is similar to the $C1_b$ structure but now also the vacant site is occupied by a X atom. They have

attracted a lot of attention due to the diverse magnetic phenomena they present [6, 26] and mainly the transition from a ferromagnetic phase to an antiferromagnetic one by changing the concentration of the carriers [27]. Webster [28] was the first to synthesise full-Heusler alloys containing Co, and Ishida and collaborators [29] have proposed that the compounds of the type Co_2MnZ , where Z stands for Si and Ge, are also half-ferromagnets. But Brown *et al.* [30] using polarized neutron diffraction measurements have shown that there is a finite very small spin-down DOS at the Fermi level instead of an absolute gap. Recently, Ambrose *et al.* managed to grow a Co_2MnGe thin film on a GaAs(001) substrate by molecular beam epitaxy [31], and Geiersbach *et al.* grew by sputtering (110) thin films of Co_2MnSi , Co_2MnGe and Co_2MnSn using a metallic seed on top of a MgO(001) substrate [32].

In this communication I study the (001) surfaces of the NiMnSb, CoMnSb and PtMnSb half-ferromagnetic materials taking into account the two different possible terminations. I compare their magnetic and electronic properties with the bulk calculations and can explain the large spin-polarisation obtained for the MnSb terminated (001) surface of NiMnSb. The second part of my study is devoted to the (001) surfaces of the Co_2MnGe and Co_2CrAl compounds. The substitution of Mn by Cr leads to a change in the electronic properties of the studied surfaces and the CrAl terminated surfaces shows a very large spin-polarisation of about 84%.

2. Method

In the calculations I used the full-potential version of the screened Korringa-Kohn-Rostoker (KKR) Green's function method [33, 34] in conjunction with the local spin-density approximation [35]. The full-potential is implemented by using a Voronoi construction of Wigner-Seitz polyhedra that fill the space [34]. I have used a two-dimensional 30×30 \mathbf{q}_{\parallel} -space grid to perform the integrations in the first surface Brillouin zone. To evaluate the charge density one has to integrate the Green's function over an energy contour in the complex energy plane; for this 42 energy points were needed. For the wavefunctions I took angular momentum up to $\ell_{max} = 3$ into account and for the charge density up to $\ell_{max} = 6$. Finally a tight-binding cluster of 51 atoms was used in the calculation of the screened KKR structure constants [36]. To simulate the surface I used a slab with 15 metal layers embedded in half-infinite vacuum from each side. Such a slab has two equivalent surfaces avoiding the creation of slab-dipoles. This slab thickness is enough so that the layers in the middle exhibit bulk properties; they show a spin-down gap of the same width as in the bulk and the same relative position of the Fermi level and finally the magnetic moments differ less than $0.01\mu_B$ from the bulk values. In figure 1 I present the structure of the (001) surfaces in the case of NiMnSb. There are two different possible terminations, one containing the Mn and Sb atoms while the other contains the Ni atom and the vacant site. In the case of the full-Heusler alloys like Co_2MnGe , there are also two possible surface terminations: the first one containing the Mn and Ge atoms in the surface layer while the second one is Co terminated (in figure 1 both the Void and Ni sites are occupied by Co atoms). The interlayer distance is 0.25 the lattice constant. I have used in all my calculations the experimental lattice constants [6]. In the perpendicular direction the layer occupancy is repeated every fourth layer, since in the $i \pm 2$ layer the atoms have exchanged positions compared to the i layer.

3. Half-Heusler Alloys

3.1. Density of states

In the first part of my study I concentrate on the half-Heusler compounds and more specifically on the (001) surfaces of the NiMnSb, CoMnSb and PtMnSb. I use the NiMnSb compound as the model system and at the end of the section I discuss its differences with the other two alloys. As already discussed in the introduction, the MnSb terminated surface of NiMnSb shows a very small reconstruction, while no information is available for the Ni-terminated surface which in principle should show a large reconstruction due to the vacant site at the surface. In my study I assume an “ideal” epitaxy in both cases. In the left panel of figure 2 I present the atom- and spin-projected density of states (DOS) for the Mn and Sb atoms in the surface layer and the Ni and vacant site in the subsurface layer for the MnSb terminated NiMnSb(001) surface, and in the right panel of the same figure I present the atom- and spin-projected DOS of the surface and the subsurface layers for the Ni terminated surface. In both cases I compare the surface DOS with the bulk calculations (dashed line) [37].

In the case of the MnSb terminated surface the DOS with the exception of the gap area is very similar to the bulk calculations. The Ni atom in the subsurface layer presents practically a half-ferromagnetic character with an almost zero spin-down DOS, while for the bulk there is an absolute gap. The spin-down band of the vacant site also presents a very small DOS around the Fermi level. The Mn and Sb atoms in the surface layer show more pronounced differences with respect to the bulk, and within the gap there is a very small Mn-*d* and Sb-*p* DOS. These states are strongly localized at the surface layer as at the subsurface layer there is practically no states inside the gap. This is in agreement with previous pseudopotentials calculations that showed that the surface states at the case of the MnSb-terminated NiMnSb(001) surface are localized at the surface layer [24]. Our results are in agreement with the experiments of Ristoiu *et al.* [21] who in the case of a MnSb well ordered (001) surface measured a high spin-polarisation.

3.2. Magnetic moments

In table 1 I have gathered the spin magnetic moments of the atoms in the surface and subsurface layers. In the case of the MnSb terminated NiMnSb(001) surface, the Ni and vacant site at the subsurface layer gain a similar charge as in the case of the bulk, $\sim 0.5e^-$ for Ni and $\sim 1.3e^-$ for the vacant site. Also the Ni and Void spin moments are comparable to the bulk situation. The Mn in the surface layer loses $\sim 0.3e^-$ more than the bulk Mn and the Sb atom loses also $\sim 0.1e^-$ more, due to the spilling out of charge into the vacuum. The spin magnetic moment of the Mn atom in the surface layer increases with respect to the bulk and reaches the $\sim 4\mu_B$. This behaviour arises from the reduced symmetry of the Mn atom in the surface which loses two of the four neighbouring Co atoms. In the majority band this leads to a narrowing of the *d*-DOS and a slight increase of the *d* count by $0.10 e^-$ due to rehybridisation, while in the minority valence band the Mn *d* contribution is decreases by $0.20 e^-$. Moreover the splitting between the unoccupied Mn states above E_F and the center of the occupied Mn states decreases and at E_F a surface states appears. I should also mention here that in the case of a half-ferromagnetic material the total spin magnetic moment per unit cell should be an integer since the number of both the total valence electrons

and the spin-down occupied states are integers; the spin moment in μ_B is simply the number of uncompensated spins. The total spin moment for the NiMnSb compound is $4 \mu_B$ (note that in the KKR method one can get the correct charge only if Lloyd's formula is used for the evaluation of the charge density. Otherwise, as it is the case in these calculations, the finite ℓ cut-off results in small numerical inaccuracies). Thus in the case of the surfaces the half-ferromagnetic character is lost and an increase of the total spin moment is observed, which is no more an integer number.

In the case of the Ni terminated surface, the changes in the DOS compared to the bulk are more pronounced. The Ni atom in the surface instead of gaining $\sim 0.5e^-$ as in the bulk now loses $\sim 0.15e^-$. Also the vacant site gains only half of the charge as in the bulk. Due to charge neutrality the Ni d bands move higher in energy. As was the case for the Mn surface atom in the MnSb terminated surface, the Ni spin magnetic moment is increased. (see table 1). The Mn and Sb atoms in the subsurface layer present a charge transfer comparable to the bulk compound and also a comparable spin moment. Within the gap there is a small Sb and Mn DOS of comparable intensity to the one of the Mn and Sb atoms at the surface layer of the MnSb terminated surface. Deeper than the the third layer from the surface the atoms regain a bulk like behaviour. The origin of the surface states is not the same for the two different terminations. In the case of the Ni terminated surface there is a practically rigid shift (although also the shape of the peaks and their intensity change) towards higher energies of the Ni bands and now the Fermi crosses a region of high DOS for both spin-directions. In the case of the MnSb terminated surface, the DOS of the Mn atom at the surface is very similar to the bulk case. The small spin-down DOS inside the gap comes from a d like atomic state of Mn that is shifted with respect to the continuum due to the lower symmetry of the surface. This peak is broadened by the interaction of the Mn atom with its neighbours, forming finally a surface band within the gap. This state is not localised only at the Mn atom but extends also to the Sb neighbouring atoms as electrons are delocalised in the two dimensions. The Ni atoms at the subsurface are slightly polarized by the Mn atoms and show a very small DOS within the gap.

3.3. Spin polarisation

As discussed in the previous paragraph, the main difference in the surface DOS between the two terminations is the different origin of the surface states. This behaviour is also reflected in the spin-polarisation of the surfaces. In table 2 I have gathered the number of spin-up and spin-down states at the Fermi level for each atom at the surface and the subsurface layer for both terminations. I calculated the spin-polarisation as the ratio between the number of spin-up states minus the number of spin-down states over the total DOS at the Fermi level. P_1 corresponds to the spin-polarisation when I take into account only the surface layer and P_2 when I also include the subsurface layer. P_2 represents quite well the experimental situation as the spin-polarisation in the case of films is usually measured by inverse photoemission which probes only the surface of the sample [38]. In all cases the inclusion of the subsurface layer increased the spin-polarisation. In the case of the Ni terminated surface, the spin-up DOS at the Fermi level is equal to the spin-down DOS and the net polarisation P_2 is zero. In the case of the MnSb terminated surface the spin-polarisation increases and now P_2 reaches a value of 38%, which means that the spin-up DOS at the Fermi level is about two times the spin-down DOS. As can be seen in table 2 the main difference between the two different terminations is the contribution of the Ni spin-down states.

In the case of the MnSb surface the Ni in the subsurface layer has a spin-down DOS at the Fermi level of 0.05 states/eV, while in the case of the Ni-terminated surface the Ni spin-down DOS at the Fermi level is 0.40 states/eV decreasing considerably the spin-polarisation for the Ni terminated surface; the Ni spin-up DOS is the same for both terminations. It is interesting also to note that for both surfaces the net Mn spin-polarisation is close to zero while Sb atoms in both cases show a large spin-polarisation and the number of the Sb spin-up states is similar to the number of Mn spin-up states, thus Sb and not Mn is responsible for the large spin-polarisation of the MnSb layer in both surface terminations. The calculated P_2 value of 38% for the MnSb terminated surface is smaller than the experimental value of 67% obtained by Ristoiu and collaborators [21] for a thin-film terminated in a MnSb stoichiometric alloy surface layer. But experimentally no exact details of the structure of the film are known and the comparison between experiment and theory is not straightforward.

3.4. *CoMnSb(001) and PtMnSb(001)*

In figure 3 I present the spin-resolved DOS for the Co and Mn atoms in the case of the two different terminated CoMnSb(001) surfaces and the Pt and Mn DOS for the PtMnSb surfaces. Both CoMnSb and PtMnSb present a behaviour similar to the NiMnSb surfaces. In the case of the MnSb terminated surfaces the DOS of the Co or Pt atom in the subsurface layer is similar to the bulk one and so does the charge transfer. The Mn and Sb atoms at the surface as was the case for the MnSb-terminated NiMnSb(001) surface show a small DOS within the gap and these states are localized at the surface layer. The atom-resolved spin moments are also close to the bulk values (see table 1) but the total spin magnetic moment is no more an integer reflecting the loss of the half-metallicity for the surfaces. As was the case for the Ni terminated surface the spin magnetic moments of the Co and Pt atoms in the case of the Pt or Co terminated surfaces, respectively, increase considerably with respect to the bulk. The Mn and Sb atoms at the subsurface layer are close to the bulk behaviour exactly as it was the case for the Ni terminated surface. It is also interesting to examine the spin-polarisation at the Fermi level. In the case of the Co terminated CoMnSb surface as it was the case for the Ni terminated surface there is a shift of the Co spin-down DOS towards higher energies and the Co spin-down DOS at the Fermi level is very high and thus P_2 is negative, meaning that the spin-down DOS is larger than the spin-up DOS at the Fermi level. In the case of the MnSb terminated CoMnSb surface, the Co atom in the subsurface layer has practically zero spin-down DOS and P_2 reaches 46%. In the case of PtMnSb, Pt does not show such a pronounced difference between the two surface terminations as the Co atom because it has practically all its d states filled and the DOS near the Fermi level is small. But also for PtMnSb the MnSb terminated surface shows a very large spin-polarisation comparable to the one of CoMnSb, while the Pt terminated (001) surface shows a positive spin-polarisation contrary to the vanishing net spin-polarisation of the Ni surface and the negative one of the Co terminated surface.

4. Full-Heusler Alloys

In the second part of my study I concentrate on the surface properties of the full-Heusler alloys containing Co. I have calculated the Co_2MnGe , Co_2MnSi and Co_2CrAl compounds. Ge and Si are isoelectronic elements and thus Co_2MnGe and Co_2MnSi

present similar properties both as bulk systems and as surfaces (they present similar magnetic moments as can be seen in table 3 and similar DOS) and therefore I only discuss the properties of Co_2MnGe . The interest on Co_2MnGe arises mainly for the fact that it is the only full-Heusler alloy that has been grown on a semiconductor [31]. Co_2MnSi has the same experimental lattice constant with GaAs and AlAs [6] and Co_2CrAl presents a very large spin-up DOS at the Fermi level due to the smaller exchange-splitting of the Cr- d states compared to the Mn- d states. Our calculations show that the bulk compounds are not really half-ferromagnets contrary to the early calculations of Ishida *et al.* using the linear-muffin tin orbitals (LMTO) method in the atomic sphere approximation [29] but the Fermi level falls within a broad region of finite very small spin-down DOS. The highest occupied bands and the lowest unoccupied bands overlap slightly destroying the indirect gap [39]. These results agree with the experimental results of Brown and collaborators [30] who using polarized neutron diffraction measurements have shown that there is a finite, but very small, DOS at the Fermi level instead of an absolute gap.

4.1. Co terminated surfaces

In table 3 I present the spin-magnetic moments for the full-Heusler alloys under study and in figure 4 the Co and Mn(Cr) DOS for the two possible terminations for the Co_2MnGe (left panel) and Co_2CrAl (right panel) compounds. I compare in all cases the surface DOS with the bulk DOS (dashed lines). In the case of the Co terminated surfaces both compounds show the same behaviour which is similar to the behaviour of the Co surface atom in the case of the Co-terminated CoMnSb surface. The lower coordination number of the Co atoms in the surface layer results in smaller covalent hybridisation between the Co spin-down d states and the Mn ones and thus there is a practically rigid shift of the spin-down Co d bands towards higher energies, and now the Fermi level falls at the edge of the large peak of the minority spin DOS. Due to this large peak it is very likely that this surface would reconstruct. The Mn and Cr atoms in the subsurface layer show now a considerable spin-down DOS within the pseudogap due to the hybridisation with the spin-down d states of the surface Co atoms. As was the case for the CoMnSb , the spin moment of the Co at the surface increases to about $1.4 \mu_B$ per Co atom while the spin moments of the Mn and Cr atoms in the subsurface layer slightly decrease due to the larger spin-down DOS around the Fermi level. Also if one adds the spin-moments for the surface and subsurface layers, the total spin magnetic moments are no more an almost integer moment due to the loss of the nearly half-metallicity. Ambrose *et al.* measured a spin magnetic moment of $5.1 \mu_B$ for a Co_2MnGe thin film [31]. This value is larger than the bulk in agreement with our results but there is no experimental information on the characterisation of the surface of the sample.

4.2. MnGe and CrAl terminated surfaces

In the case of the MnGe terminated Co_2MnGe (001) surface the behaviour is similar to the MnSb terminated surface in the CoMnSb compound. Due to the reduced symmetry (Mn loses two out of the four Co nearest neighbours) the hybridisation between the Mn minority d states and the Co ones is reduced, leading to an increase of the Mn spin-moment by about $0.6 \mu_B$, while the Co atom at the subsurface layer behaves similar to the bulk case. Where the Mn pseudogap was located in the bulk,

there is now a small peak due to a d like Mn atomic state that is shifted in energy due to the lower symmetry and which is pinned at the Fermi level. This state although located at the surface layer is not well localised and the Co atoms in the subsurface layer present a similar peak at the Fermi level. Ishida *et al.* [40] have studied the MnSi and MnGe terminated Co_2MnSi and Co_2MnGe surfaces using a 13 layers thick film. They claim that in the case of the MnSi surface the half-ferromagnetic character, which they have calculated for the bulk Co_2MnSi [29], is preserved, while in the case of the MnGe surface, surface states destroy the gap (in the paper they present the results for the MnSi surface and only shortly refer to the MnGe surface). These results are peculiar since they get a similar electronic structure for the bulk compounds and there is no obvious reason obliging only the MnGe surface to present surface states. Mn atoms have the same environment in both cases and the hybridisation between Mn and the sp atoms is similar for both Ge and Si. A plausible reason for this behaviour is the use of the atomic-sphere approximation in their calculations, where the potential and the charge density are supposed to be spherically symmetric. Although this approximation can accurately describe the bulk compounds due to the close-packed structure they adopt, it is not suitable for surfaces where the non-spherical contributions to the potential and the charge density are important.

The case of Co_2CrAl is different from Co_2MnGe . In line with the reduction of the total valence electrons by 2, the Cr moment is rather small ($1.54 \mu_B$) yielding a total moment of only $3 \mu_B$ instead of $5 \mu_B$ for Co_2MnGe . The Co terminated $\text{Co}_2\text{CrAl}(001)$ surface shows a similar behaviour as the corresponding surface of Co_2MnGe , being in both cases dominated by a strong Co peak in the gap region of the minority band. However the CrAl terminated Co_2CrAl surface behaves very differently, being driven by the large surface enhancement of the Cr moment from $1.54 \mu_B$ to $3.12 \mu_B$. As a consequence the splitting of the Cr peaks in the majority and minority bands is even enlarged and in particular in the minority band the pseudogap is preserved. Thus this surface is a rare case, since for all the other surfaces studied in this paper, the half-metallicity is destroyed by surface states.

4.3. Spin polarisation

In the last part of my study I will discuss the spin-polarisation for the surfaces of the full-Heusler alloys. I will concentrate on the MnGe and CrAl terminated surfaces as the Co-terminated ones might show large reconstructions and thus are not interesting for applications. In table 4 I present the atom-resolved spin-up and spin-down DOS at the Fermi level and the obtained spin-polarisation. In the case of the MnGe terminated surface the surface states completely kill the spin polarisation as the majority spin DOS is pretty small. In the case of the CrAl terminated surface the situation is completely different. The minority DOS around the Fermi level is the same for both the bulk and the CrAl surface. The Fermi level falls within a region of very high Cr and Co majority spin DOS as can be seen in table 4 and thus 92% of the electrons at the Fermi level are of spin-up character and P_2 reaches 84%.

5. Summary

I have performed *ab-initio* calculations based on the full-potential version of the screened KKR Green's function method for the (001) surfaces of a series of half-ferromagnetic Heusler alloys, *i.e.* for the half-Heuslers NiMnSb, CoMnSb and PtMnSb

with the $C1_b$ structure and the full-Heuslers Co_2MnGe , Co_2MnSi and Co_2CrAl with the $L2_1$ structure. For the half-Heusler alloys, the MnSb terminated (001) surfaces present electronic and magnetic properties similar to the bulk compounds. There is however a small finite Mn- d and Sb- p DOS within the bulk spin-down gap and these surface states are strongly localized at the surface layer. The spin-polarisation at the Fermi level for this termination reaches the 38%. The (001) surfaces terminated at Ni, Co or Pt present a quite large density of states at the Fermi level and properties considerably different from the bulk and the MnSb terminated surfaces. In the case of the Co-based full-Heusler alloys, the Co terminated surfaces show a behaviour similar to the Co terminated CoMnSb surface and the Co minority states shift practically in a rigid way towards higher energies, destroying the pseudogap. In the case of the MnGe terminated $\text{Co}_2\text{MnGe}(001)$ surfaces, the surface states kill completely the spin polarisation but in the case of CrAl the combination of the very high majority-spin Cr and Co DOS and the absence of surface states within the pseudogap result in a very high spin-polarisation of around 84%. Thus of all the investigated surfaces, this is the only one which preserves the nearly half-metallicity at the surface.

Acknowledgments

The author acknowledges financial support from the RT Network of *Computational Magneto-electronics* (contract RTN1-1999-00145) of the European Commission. The author would like also to thank professor P. H. Dederichs for helpful discussions and for a critical reading of the manuscript.

References

- [1] Baibich M N, Broto J M, Fert A, Nguyen Van Dau F, Petroff F, Etienne P, Creuzet G, Friederich A and Chazelas J 1988 *Phys. Rev. Lett.* **61** 2472
- [2] Binasch G, Grünberg P, Saurenbach F and Zinn W 1989 *Phys. Rev. B* **39** 4828
- [3] Kilian K A and Victora R H 2000 *J. Appl. Phys.* **87** 7064; Kilian K A and Victora R H 2001 *IEEE Trans. Magn.* **37** 1976
- [4] Tanaka C T, Nowak J and Moodera J S 1999 *J. Appl. Phys.* **86** 6239
- [5] Caballero J A, Park Y D, Childress J R, Bass J, Chiang W -C, Reilly A C, Pratt Jr W P and Petroff F 1998 *J. Vac. Sci. Technol. A* **16** 1801; Hordequin C, Nozières J P and Pierre J 1998 *J. Magn. Magn. Mater.* **183** 225
- [6] Webster P J and Ziebeck K R A, in *Alloys and Compounds of d-Elements with Main Group Elements. Part 2.*, edited by H.R.J. Wijn, Landolt-Börnstein, New Series, Group III, Vol. 19, Pt.c (Springer-Verlag, Berlin), pp. 75-184.
- [7] de Groot R A, Mueller F M, van Engen P G and Buschow K H J 1983 *Phys. Rev. Lett.* **50** 2024
- [8] Galanakis I, Ostanin S, Alouani M, Dreyssé H and Wills J M (2000) *Phys. Rev. B* **61** 4093
- [9] Youn S J and Min B I 1995 *Phys. Rev. B* **51** 10436
- [10] Kübler J 1984 *Physica B* **127** 257
- [11] Kirillova M N, Makhnev A A, Shreder E I, Dyakina V P and Gorina N B 1995 *Phys. Status Solidi (b)* **187** 231
- [12] Hanssen K E H M and Mijnders P E 1990 *Phys. Rev. B* **34** 5009; Hanssen K E H M, Mijnders P E, Rabou L P L M and K.H.J. Buschow K H J 1990 *Phys. Rev. B* **42** 1533
- [13] Bobo J F, Johnson R J, Kautzky M, Mancoff F B, Tuncel E, White R L and Clemens B M 1997 *J. Appl. Phys.* **81** 4164
- [14] van Roy W, de Boeck J, Brijns B and Borghs G 2000 *Appl. Phys. Lett.* **77** 4190; van Roy W, Borghs G and de Boeck J 2001 *J. Cryst. Growth* **227-228** 862; Schlomka J -P, Press W, Fitzsimmons M R, Lütt M and Grigorov I 1998 *Physica B* **248** 140; Schlomka J -P, Tolan M and Press W 2000 *Appl. Phys. Lett.* **76** 2005
- [15] Soulen Jr R J, Byers J M, Osofsky M S, Nadgorny B, Ambrose T, Cheng S F, Broussard P R, Tanaka C T, Nowak J, Moodera J S, Barry A and Coey J M D 1998 *Science* **282** 85
- [16] Mancoff F B, Clemens B M, Singley E J and Basov D N 1999 *Phys. Rev. B* **60** R12565

- [17] Zhu W, Sinkovic B, Vescovo E, Tanaka C and Moodera J S 2001 *Phys. Rev. B* **64** R060403
- [18] Bona G L, Meier F, Taborelli M, Bucher E and Schmidt P H 1985 *Solid State Commun.* **56** 391
- [19] Caballero J A, Reilly A C, Hao Y, Bass J, Pratt W P, Petroff F and Childress 1999 *J. Magn. Mater.* **198-199** 55; Kabani R, Terada M, Roshko A and Moodera J S 1990 *J. Appl. Phys.* **67** 4898
- [20] Tanaka C T, Nowak J and Moodera J S 1997 *J. Appl. Phys.* **81** 5515
- [21] Ristoiu D, Nozières J P, Borca C N, Komesu T, Jeong H -K and Dowben P A 2000 *Europhys. Lett.* **49** 624; Ristoiu D, Nozières J P, Borca C N, Borca B and Dowben P A 2000 *Appl. Phys. Lett.* **76** 2349; Borca C N, Komesu T, Jeong H -K, Dowben P A, Ristoiu D, Hordequin Ch, Pierre J and Nozières J P 2000 *Appl. Phys. Lett.* **77** 88
- [22] Borca C N, Komesu T, Jeong H -K, Dowben P A, Ristoiu D, Hordequin Ch, Nozières J P, Pierre J, Stadler Sh and Idzerda Y U 2001 *Phys. Rev. B* **64** 052409
- [23] Wijs G A and de Groot R A 2001 *Phys. Rev. B* **64** R020402
- [24] Jenkins S J and King D A 2001 *Surf. Sci.* **494** L793
- [25] Jenkins S J and King D A 2002 *Surf. Sci.* **501** L185
- [26] Pierre J, Skolozdra R V, Tobola J, Kaprzyk S, Hordequin C, Kouacou M A, Karla I, Currat R and Lelièvre-Berna E 1997 *J. Alloys Comp.* **262-263** 101; Tobola J and Pierre J 2000 *J. Alloys Comp.* **296** 243
- [27] Kübler J, Williams A R and Sommers C B 1983 *Phys. Rev. B* **28** 1745
- [28] Webster P J 1971 *J. Phys. Chem. Solids* **32** 1221
- [29] Ishida S, Akazawa S, Kubo Y and Ishida J 1982 *J. Phys. F: Met. Phys.* **12** 1111; Ishida S, Fujii S, Kashiwagi S and Asano S 1995 *J. Phys. Soc. Japan* **64** 2152
- [30] Brown P J, Neumann K U, Webster P J and Ziebeck K R A 2000 *J. Phys.: Condens. Matter* **12** 1827
- [31] Ambrose T, Krebs J J and Prinz G A 2000 *Appl. Phys. Lett.* **76** 3280; Ambrose T, Krebs J J and Prinz G A 2000 *J. Appl. Phys.* **87** 5463
- [32] Geiersbach U, Bergmann A and Westerholt K *J. Magn. Mater.* to be published
- [33] Zeller R, Dederichs P H, Újfalussy B, Szunyogh L and Weinberger P 1995 *Phys. Rev. B* **52** 8807
- [34] Papanikolaou N, Zeller R and Dederichs P H 2002 *J. Phys.: Condens. Matter* **14** 2799
- [35] Vosko S H, Wilk L and Nusair N 1980 *Can. J. Phys.* **58** 1200
- [36] Zeller R 1997 *Phys. Rev. B* **55** 9400
- [37] Galanakis I, Dederichs P H and Papanikolaou N arXiv:cond-mat/0203534
- [38] Borca C N, Komesu T and Dowben P A 2002 *J. Electron Spectrosc. Relat. Phenom.* **122** 259
- [39] A detailed study of the full-Heusler alloys would be presented elsewhere.
- [40] Ishida S, Masaki T, Fujii S and Asano S 1998 *Physica B* **245** 1

Table 1. Spin moments in μ_B for the Ni-, Pt- and CoMnSb compounds in the case of i) bulk compounds; ii) the Mn and Sb atoms in the surface and the Ni (Pt, Co) and the vacant site in the subsurface layer for the MnSb-terminated (001) surfaces; iii) like (ii) for the Ni, Pt or Co terminated surfaces. For the surfaces the “total” moment denotes the sum of the moments in the surface and subsurface layers.

$m^{spin}(\mu_B)$		Ni (Pt, Co)	Mn	Sb	Void	Total
NiMnSb	Bulk	0.26	3.70	-0.06	0.05	3.96
	(001)MnSb	0.22	4.02	-0.10	0.04	4.19
	(001)Ni	0.46	3.84	-0.05	0.05	4.30
PtMnSb	Bulk	0.09	3.89	-0.08	0.04	3.94
	(001)MnSb	0.08	4.19	-0.13	0.03	4.17
	(001)Pt	0.27	4.15	-0.04	0.04	4.42
CoMnSb	Bulk	-0.13	3.18	-0.10	0.01	2.96
	(001)MnSb	-0.06	3.83	-0.12	0.01	3.65
	(001)Co	1.19	3.31	-0.09	0.02	4.43

Table 2. Atomic-resolved spin-up and spin-down DOS at the Fermi level in states/eV units. They are presented as ratios spin-up over spin-down. Polarization ratios at the Fermi level are calculated taking into account only the surface layer P_1 , and both the surface and subsurface layers P_2 .

MnSb-termination						
	Surface Layer		Subsurface Layer		P_1 ($\frac{\uparrow-\downarrow}{\uparrow+\downarrow}$)	P_2 ($\frac{\uparrow-\downarrow}{\uparrow+\downarrow}$)
	Mn (\uparrow / \downarrow)	Sb (\uparrow / \downarrow)	Ni[Co,Pt] (\uparrow / \downarrow)	Void (\uparrow / \downarrow)		
NiMnSb	0.16/0.19	0.17/0.03	0.28/0.05	0.05/0.02	26%	38%
CoMnSb	0.23/0.27	0.16/0.07	0.91/0.15	0.07/0.02	6%	46%
PtMnSb	0.21/0.24	0.31/0.06	0.38/0.04	0.08/0.02	26%	46%
Ni(Co,Pt)Void-termination						
	Subsurface Layer		Surface Layer		P_1 ($\frac{\uparrow-\downarrow}{\uparrow+\downarrow}$)	P_2 ($\frac{\uparrow-\downarrow}{\uparrow+\downarrow}$)
	Mn (\uparrow / \downarrow)	Sb (\uparrow / \downarrow)	Ni[Co,Pt] (\uparrow / \downarrow)	Void (\uparrow / \downarrow)		
NiMnSb	0.18/0.16	0.13/0.05	0.27/0.40	0.04/0.02	-16%	0%
CoMnSb	0.55/0.68	0.12/0.07	0.54/1.15	0.05/0.04	-34%	-22%
PtMnSb	0.18/0.14	0.21/0.07	0.30/0.24	0.05/0.02	14%	22%

Table 3. Spin moments in μ_B for the Co_2MnGe , Co_2MnSi and Co_2CrAl compounds in the case of i) bulk compounds; ii) the Mn(Cr) and Ge(Si,Al) atoms in the surface and the Co atoms in the subsurface layer for the MnGe(MnSi,CrAl)-terminated (001) surfaces; iii) like (ii) for the Co terminated surfaces. For the surfaces the “total” moment denotes the sum of the moments in the surface and subsurface layers.

$m^{spin}(\mu_B)$		Co	Mn(Cr)	Ge(Si,Al)	Total
Co_2MnGe	Bulk	0.98	3.04	-0.06	4.94
	(001)MnGe	0.96	3.65	-0.10	5.47
	(001)Co	1.40	2.85	-0.09	5.56
Co_2MnSi	Bulk	1.02	2.97	-0.07	4.94
	(001)MnSi	0.95	3.56	-0.13	5.33
	(001)Co	1.29	2.72	-0.11	5.19
Co_2CrAl	Bulk	0.76	1.54	-0.10	2.96
	(001)CrAl	0.76	3.12	-0.02	4.62
	(001)Co	1.36	1.06	-0.11	3.67

Table 4. Same as Table 2 for the MnGe and CrAl terminated (001) surfaces of the Co_2MnGe and Co_2CrAl compounds, respectively.

MnGe and CrAl terminations		
	Co_2MnGe	Co_2CrAl
Mn-Cr (\uparrow / \downarrow)	0.26/0.30	1.48/0.03
Ge-Al (\uparrow / \downarrow)	0.22/0.18	0.01/0.15
Co (\uparrow / \downarrow)	0.41/0.48	1.03/0.06
P_1 ($\begin{smallmatrix} \uparrow \\ \downarrow \\ \uparrow \\ \downarrow \end{smallmatrix}$)	0%	78%
P_2 ($\begin{smallmatrix} \uparrow \\ \downarrow \\ \downarrow \\ \uparrow \end{smallmatrix}$)	-6%	84%

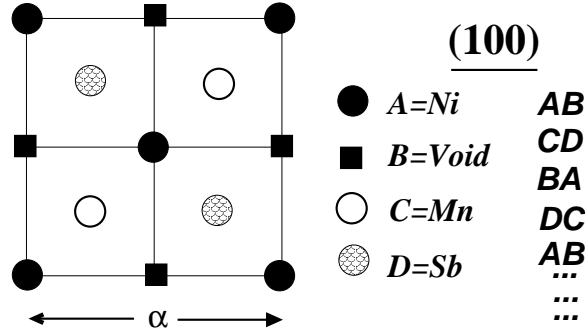


Figure 1. Schematical representation of the (001) surface of NiMnSb. There are two possible terminations: i) MnSb and ii) Ni-Void. The interlayer distance is $0.25a$. In the $i \pm 2$ layer the atoms have exchanged positions compared to the i layer. In the case of the Co_2MnGe compound the Co atoms occupy the Ni and Void sites.

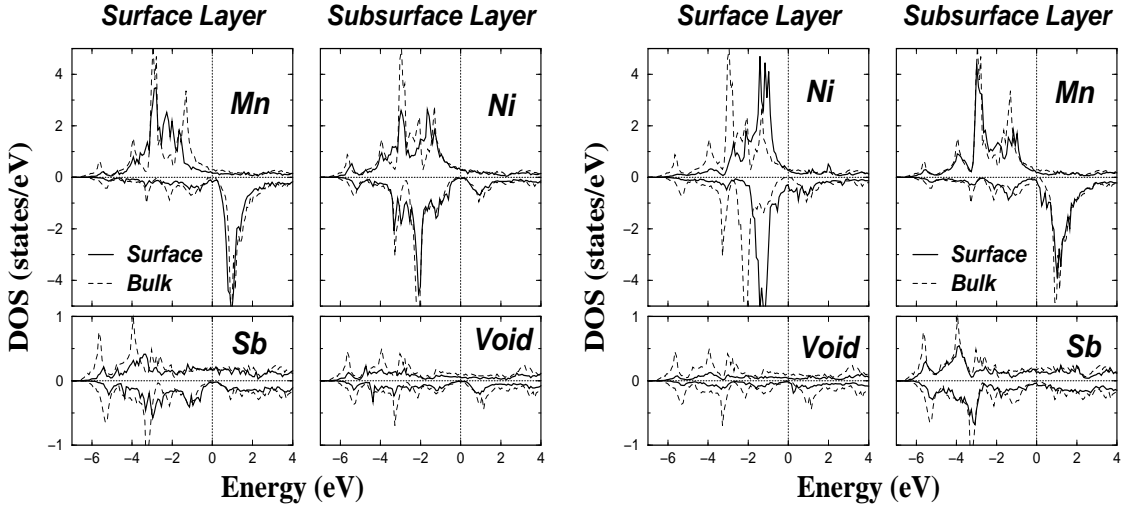


Figure 2. Spin- and atom-projected DOS for the MnSb-terminated NiMnSb(001) surface (left panel) and for the Ni-Void terminated (001) surface (right panel). The dashed lines give the local DOS of the atoms in the bulk.

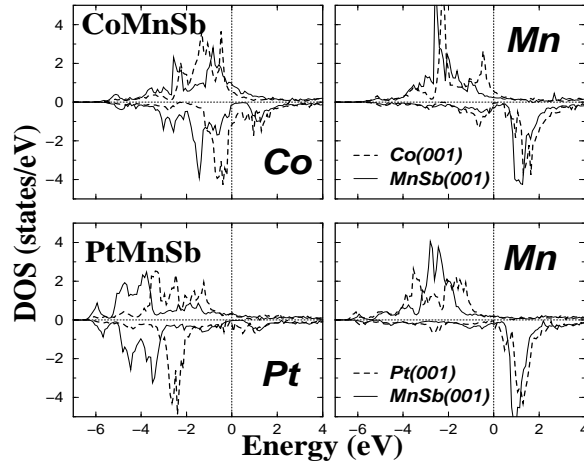


Figure 3. In the upper panel the spin-resolved DOS for Co in the surface layer and Mn in the subsurface layer in the case of the Co-terminated CoMnSb(001) surface and for Co in the subsurface layer and Mn in the surface layer for a MnSb-terminated CoMnSb(001) surface. In the bottom panel the spin-resolved DOS of the PtMnSb surface for the Pt and MnSb terminations are given.

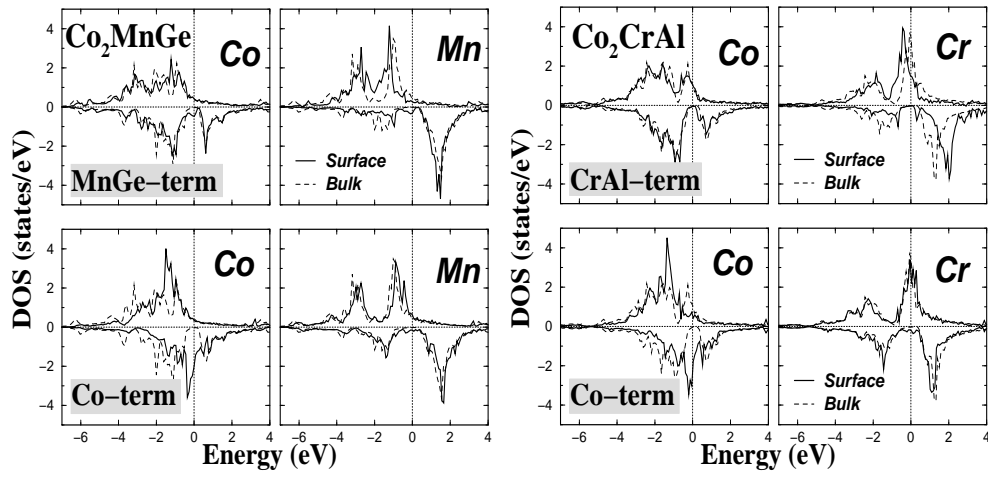


Figure 4. Atom- and spin-projected DOS for the Mn atom in the surface and the Co atom in the subsurface layer in the case of the MnGe terminated Co_2MnGe (001) surface (left upper panel) and the Co atom in the surface layer and the Mn atom in the subsurface for the Co terminated surface (left bottom panel). In the right panel similar DOS for the Co_2CrAl compound. With dashed line the bulk results.